



## Supplementary Information for

### **Cerebral Cortical Folding, Parcellation, and Connectivity in Humans, Nonhuman Primates, and Mice**

David C. Van Essen, Chad J. Donahue, Timothy S. Coalson, Henry Kennedy,  
Takuya Hayashi, Matthew F. Glasser

Corresponding author: David C. Van Essen

Email: [vanessen@wustl.edu](mailto:vanessen@wustl.edu)

#### **This PDF file includes:**

Supplementary text

Figs. S1 to S3

References for SI reference citations

## Supplementary Information Text

**Overview of supplementary figures.** Supplementary figures S1 – S3 illustrate important aspects of individual variability of cortical folding in three species.

Fig. S1 and S2 together demonstrate that the extent of folding variability between individuals (and also between the left and right hemispheres of the same individual) scales with brain size and complexity of convolutions. Fig. S1 illustrates this using volumetric methods, namely, axial T1w MRI slices through individual and group-average volumes aligned by nonlinear registration. The results suggest that variability is low in macaques, intermediate in chimpanzees and high in humans. Fig. S2 shows that these observations on gross morphological variability and bilateral symmetry can be analyzed and visualized more clearly using cortical surface models and surface-based registration to a group-average atlas. Fig. S3 provides evidence that the main differences between human and nonhuman group average surfaces are not attributable to the different numbers of subjects contributing to each atlas.

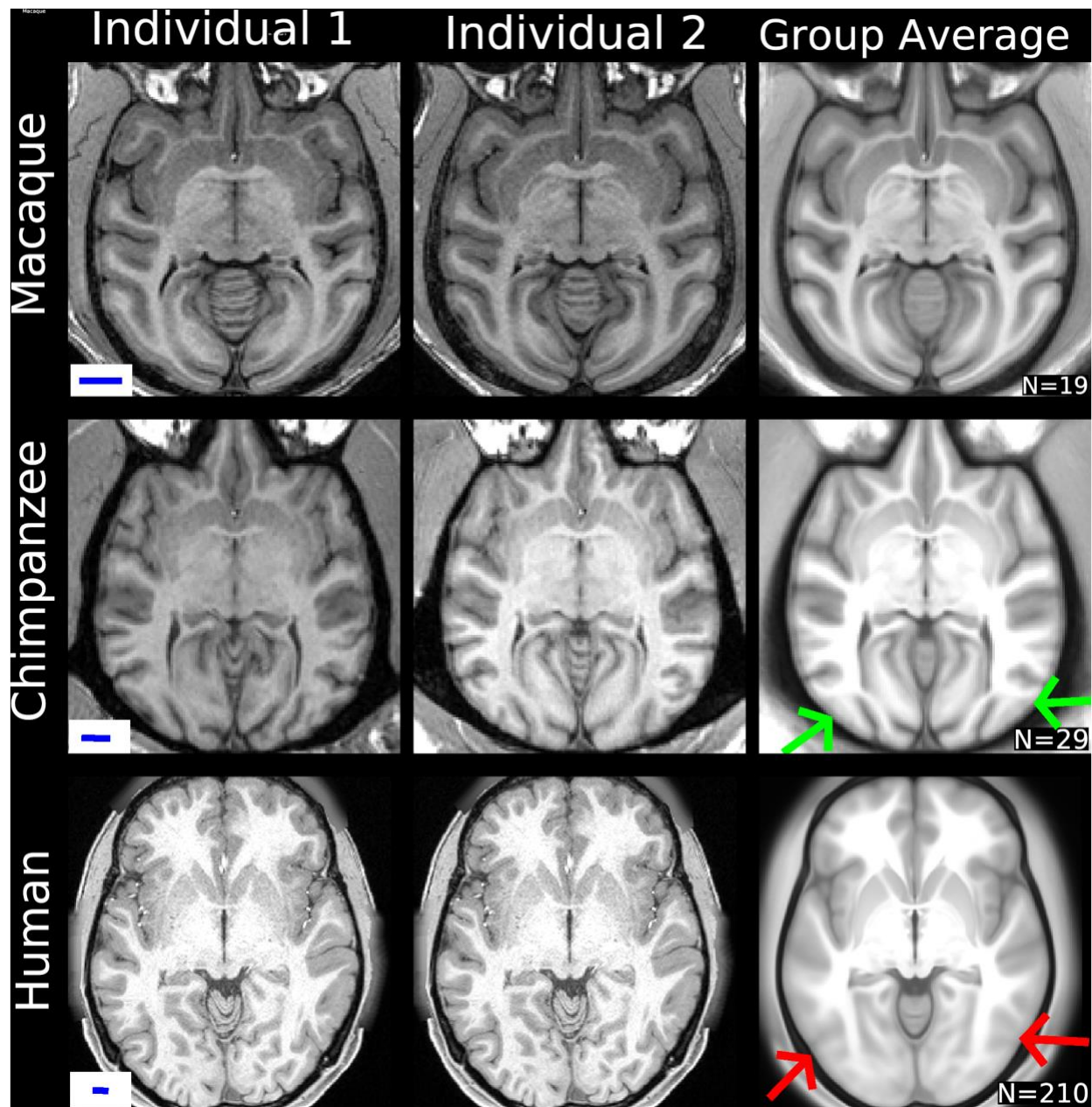


Fig. S1. Individual variability in structural MRI volume slices. Left and center columns: individual-subject axial T1-weighted MRI slices after rigidly aligning each native scan to a standard orientation in 3D space for macaque (top row), chimpanzee (middle row) and human (bottom row). Right column: population-average atlas volumes (N=19 for macaque Yerkes19\_v1.2; N=29 for chimpanzee Yerkes29\_v1.2; N=210 for human HCP Q1-Q6\_RelatedValidation210), all generated by iterative nonlinear registration using FSL's FNIRT algorithm. Scale bars (1 cm) on the left apply to all images in that row. In the macaque, the thickness and the pattern of cortical gray matter folding is comparable in the population average volume to that in individual scans, reflecting the consistency of folding across individuals. Further, the left and right hemisphere images are relatively symmetric by visual inspection. In the chimpanzee, the population average volume is slightly blurry in several cortical regions (green arrows) and is blurrier still in

parts of the human population average (red arrows). The increased blurring arises because nonlinear volume-registration algorithms fail to align tissue boundaries between gray and white matter and cerebrospinal fluid in regions of high folding variability, as they do not take advantage of the topology of the cortical sheet (1). In terms of bilateral symmetry, the left and right hemispheres of individual chimpanzees and humans show many differences, but the population average volumes are relatively symmetric in both species. Data are available at <https://balsa.wustl.edu/kN6rD>

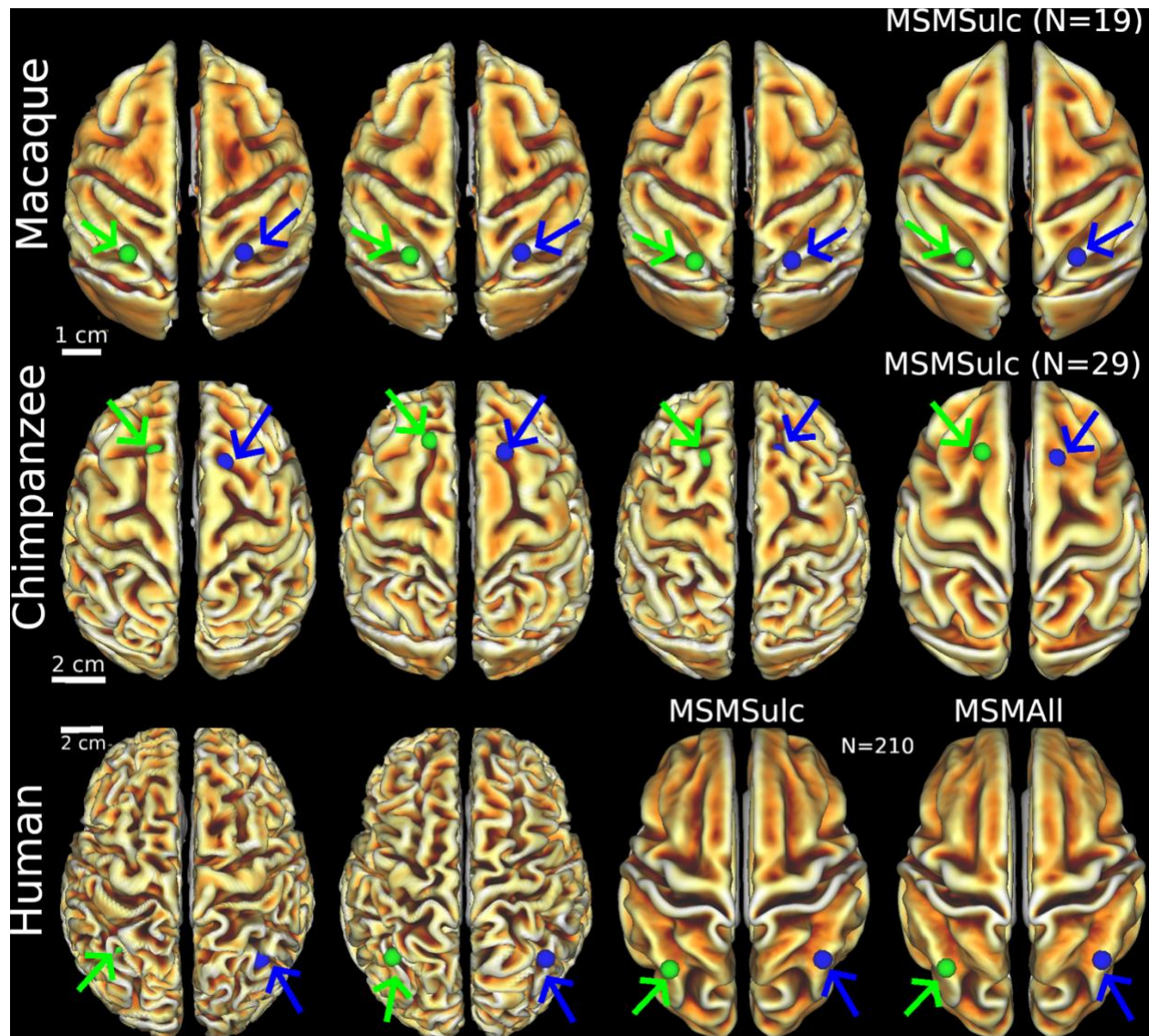


Fig. S2. Individual variability of cortical folding shown on dorsal views of cortical midthickness surface reconstructions and surface-based registration to an atlas, using MSMSulc folding-based registration for all 3 species (2,3) and also MSMAII areal feature based registration for humans (4,5). Scale bars (2 cm) on left apply to all individuals in that row. In the top row, the left and right midthickness surfaces for the three individual macaques are highly similar in shape except for local irregularities reflecting minor segmentation artifacts. The Yerkes19 group-average left and right midthickness surfaces (top right, aligned using folding features) are slightly smoother but otherwise nearly identical to the individuals. The strong bilateral symmetry in the group average surfaces was used to generate standard-mesh representations that have excellent left-right geographic correspondence (4) using GIFTI and CIFTI data formats (6). For example, the blue vertex identified on the right group average inferior parietal lobule lies in precisely corresponding locations in all three individual right hemispheres (blue vertices, arrows) and in closely corresponding locations in the left hemisphere atlas and individuals (green vertices, arrows). For the chimpanzee (middle row), folding differences among individuals are more pronounced, as are the differences between the Yerkes29 group average atlas surface and the individuals (aligned using folding). All primary and secondary gyri and sulci visible in the

individuals are discernible in the group average surfaces, but some sulci are shallower in the atlas. For example, the highlighted vertex in the shallow superior frontal sulcus of the group average, lies deep within a sulcus in some hemispheres but near a gyral crown in others (blue and green vertices and arrows). For humans (bottom row), individual differences in cortical folding are even more pronounced. The 210V group average midthickness surfaces aligned using cortical folding ('MSMSulc', third column) differ markedly from any individual in a region-specific manner. Near early sensory areas (e.g., the central sulcus), folding patterns are relatively consistent, and sulci are deep in the atlas surfaces. In highly variable cognitive regions, the average surface is smoother and intermediate in depth relative to individual-subject folds (blue and green vertices, arrows in the inferior parietal lobule). When intersubject registration is constrained by areal features based on myelin maps and functional MRI (fMRI) using 'MSMAII' (fourth column), the average midthickness surface is even smoother because cortical areas vary in location relative to cortical folds (1). MSMSulc and MSMAII average midthickness surfaces both show high bilateral symmetry, which is critical for establishing left-right correspondences (7). Data are available at <https://balsa.wustl.edu/0LrDm>, <https://balsa.wustl.edu/2VmlN>, <https://balsa.wustl.edu/rrgVI>

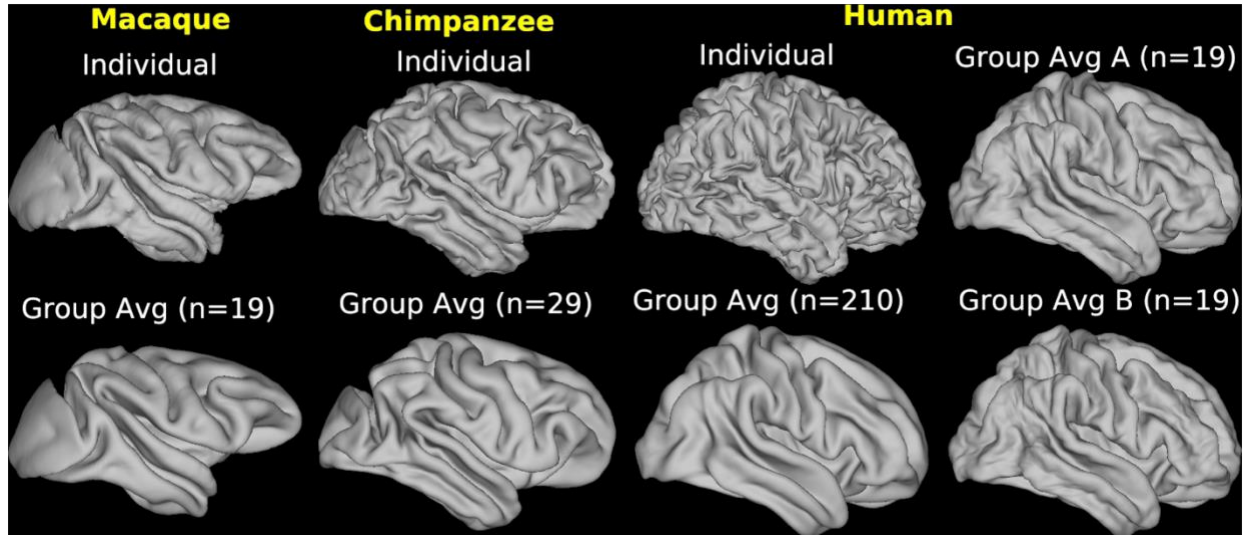


Fig. S3. Effects of sample size on human group average surfaces. The species differences shown in Fig. S2 in the smoothness of group average surfaces might in principle be due in part to the order of magnitude difference in the number of subjects contributing to the macaque ( $n = 19$ ), chimpanzee ( $n = 29$ ) and human ( $n = 210$ ). To address this issue, we generated two additional group average human right hemisphere surfaces, each based on a different group of 19 subjects, as shown on the far right. These 19-subject group averages surfaces are similar in shape to one another and to the 210V group average (third column) in terms of major gyral and sulcal features, but they each have many local surface irregularities that reflect incomplete averaging of features in regions of high folding variability. The group average macaque and chimpanzee surfaces lack such prominent local irregularities and are closer in shape to the individual subjects. This argues that different numbers of subjects need to be averaged in each species to achieve consistency in the group average surfaces, owing to species differences in the degree of individual variability. Put another way, many more human surfaces must be included in order to generate surfaces comparably as smooth as the chimpanzee or macaque average surfaces. Data are available at <https://balsa.wustl.edu/g71Gm>

### Supplementary References.

1. Coalson TS, Van Essen DC, & Glasser MF (2018) The impact of traditional neuroimaging methods on the spatial localization of cortical areas. *Proc Natl Acad Sci U S A* 115(27):E6356-E6365.
2. Donahue CJ, Glasser MF, Preuss TM, Rilling JK, & Van Essen DC (2018) A quantitative assessment of prefrontal cortex in humans relative to nonhuman primates. *Proc Natl Acad Sci* 115:E5183-E5192.
3. Glasser MF, *et al.* (2016a) A multi-modal parcellation of human cerebral cortex. *Nature* 536(7615):171-178.
4. Van Essen DC, Glasser, M.F., Dierker, D. and Harwell, J. (2012) Cortical parcellations of the Macaque monkey analyzed on surface-based atlases. *Cereb Cortex* 22:2227-2240. doi 2210.1093/cercor/bhr2290.
5. Robinson EC, *et al.* (2018) Multimodal surface matching with higher-order smoothness constraints. *Neuroimage* 167:453-465.
6. Glasser MF, *et al.* (2013) The minimal preprocessing pipelines for the Human Connectome Project. . *Neuroimage* 80:105-124
7. Van Essen DC, Glasser MF, Dierker DL, Harwell J, & Coalson T (2012) Parcellations and hemispheric asymmetries of human cerebral cortex analyzed on surface-based atlases. *Cereb Cortex* 22(10):2241-2262.